



HAL
open science

New features in the Raman spectrum of Silica: Key-points in the improvement on structure knowledge

M. Chligui, G. Guimbretiere, A. Canizares, G. Matzen, Y. Vaills, Patrick
Simon

► **To cite this version:**

M. Chligui, G. Guimbretiere, A. Canizares, G. Matzen, Y. Vaills, et al.. New features in the Raman spectrum of Silica: Key-points in the improvement on structure knowledge. 2010. hal-00520823

HAL Id: hal-00520823

<https://hal.science/hal-00520823v1>

Preprint submitted on 24 Sep 2010

HAL is a multi-disciplinary open access archive for the deposit and dissemination of scientific research documents, whether they are published or not. The documents may come from teaching and research institutions in France or abroad, or from public or private research centers.

L'archive ouverte pluridisciplinaire **HAL**, est destinée au dépôt et à la diffusion de documents scientifiques de niveau recherche, publiés ou non, émanant des établissements d'enseignement et de recherche français ou étrangers, des laboratoires publics ou privés.

New features in the Raman spectrum of Silica: Key-points in the improvement on structure knowledge

M. Chligui, G. Guimbretière, A. Canizarès, G. Matzen, Y. Vaills, P. Simon

CNRS/CEMHTI UPR3079, 1D Avenue de la Recherche Scientifique, 45071 Orléans, France, and

Université d'Orléans, 45067 Orléans Cedex 2, France

This paper reports the evidence of new signatures in the low-frequency Raman spectrum of silica, obtained by very high signal-to-noise experiments. Two new Raman lines are observed at 295 and 380 cm^{-1} , and the presence of a third one at 245 cm^{-1} is needed to account for the experimental spectra. The origin of these supplementary lines is discussed in terms of n -membered rings of $[\text{SiO}_{4/2}]$ tetrahedral entities inside the glassy network.

Amorphous silica (SiO_2) is one beyond the most-well known materials, with interests going from a model compound in glass physics up to numerous industrial applications for optics and electronics. A huge number of papers devoted to it stands in the literature, in such a point that its structure and dynamics look well-known and are then used as reference for the study of more complex systems. Raman scattering investigations for instance are numerous and it is then difficult today to identify the first report on silica. The Raman spectrum of silica is today rather well understood since the works by Galeener and Lucovsky thirty years ago^{1,2} and confirmed by subsequent ab-initio calculations³. The low-wavenumbers region of the silica Raman spectrum in the VV configuration polarization is usually decomposed as made of the boson peak at low wavenumbers (pointing around 50 cm^{-1}), a broad and asymmetric band at 450 cm^{-1} assigned to δ_{bend} (SiOSi) bending vibrations (frequently referred as R-band), plus the D_1 and D_2 narrow peaks closed to 495 and 600 cm^{-1} . One widely accepted view of the structure of silica is a disordered more or less open network of corner-linked interconnected $[\text{SiO}_{4/2}]$ tetrahedral entities. Such view intrinsically considers the existence of $[\text{SiO}_{4/2}]$ membered rings (hereafter denoted MR), and as an evidence, the so-called D_1 and D_2 peaks are now unambiguously assigned to respectively four-tetrahedral (4-MR) and three-tetrahedra membered rings (3-MR). The specific dynamics of these MR was recently observed⁴ by picosecond spectroscopy, that confirms the strong decoupling of these vibrations from the whole silica network. Nevertheless these assignments remain partially discussed,⁵ with possible mixed influence of 3-MR and 4-MR in the D_1 band⁶

and the absence of consensus in the estimation of rings population^{7, 6, 8-9}. Raman spectroscopy offers then a simple way to probe the statistics for 3 and 4 –MR, and the greatest part of the literature devoted to rings statistics has focused on these small rings. However, the population of 3- and 4-MR is not dominant in silica compared to the whole MR distribution that can be obtained by molecular dynamics⁷. Unfortunately, larger MR are rather hardly experimentally accessible, and very few knowledge is available on them apart from numerical approaches. In the literature one can find also some descriptions of the (SiOSi) bridges dynamic by force constant models^{10, 11}. These rather simple models link vibrational spectroscopic data with the average angle θ and effective forces constant of (SiOSi). From considerations of these models, the Raman signatures of 5-MR and 6-MR larger rings are expected to be at lower wavenumbers than for small rings, i.e., in the R-band region. Besides, independently of any specific ring patterns consideration, three different spectral features were suggested¹² to compose part of the isotropic R-band (symmetric stretching involving (SiOSi) bridges, δ_{scis} scissoring of $[\text{SiO}_{4/2}]$, and Δ_{scis} scissoring of the $[\text{SiO}_{4/2}]$ - $[\text{Si}_{4/4}]$ extended tetrahedron). Therefore, it is not surprising that the R-band is sometimes described as the superposition of several individual symmetric bands (see for instance¹³), but the proposed decompositions remain a little bit ambiguous as different band combinations can reproduce the broad experimental asymmetric shape, due to lack of any pointed inflexion point on the rising edge between 200 and 400 cm^{-1} .

This short paper reports very high signal-to-noise Raman spectra of silica that highlights new structuring in the broad asymmetric 450 cm^{-1} R-band. These new features closed to 295 and 380 cm^{-1} are observed here for the first time in the nonetheless well know spectrum of silica. They arise owing to increase of the signal-to-noise ratio and have to be considered after a rigorous and exhaustive study, in order to exclude any instrumental origin. So, in the following, we present first the experimental condition leading to the new spectral features observation. Next, we introduce and illustrate in a short discussion, the relevant consequence of such observations in the study of vitreous silicates structure by mean of Raman spectroscopy.

Experiments were done on two spectrometers: a Renishaw Invia Reflex with a Leica DM 2500 microscope (simple spectrometer configuration), and a Jobin-Yvon T64000 (triple subtractive configuration), in macro configuration. Both systems are multichannel ones with CCD detectors. Different excitation laser wavelengths were used: 457 , 514 (Ar^+ lines) and 633 nm (He-Ne line). Measurements with the Leica microscope were done with two objectives in order to check the effect of numerical aperture and the subsequent changes in light polarization. The specificities of the experiments reported here are the very long acquisition times (up to 20 hours), in order to substantially increase the signal-to-noise ratio. As in this case the saturation limit of the CCD detector can be attained, measurements were performed in accumulation mode (several subsequent spectra of lower time, to keep beyond the saturation limit, which are added at the end of experiment). Silica samples were of Corning 7980 type. A test was done on a 7980 sample, thermally treated to change the fictive temperature (Corning 7980 T_f is 1040°C).

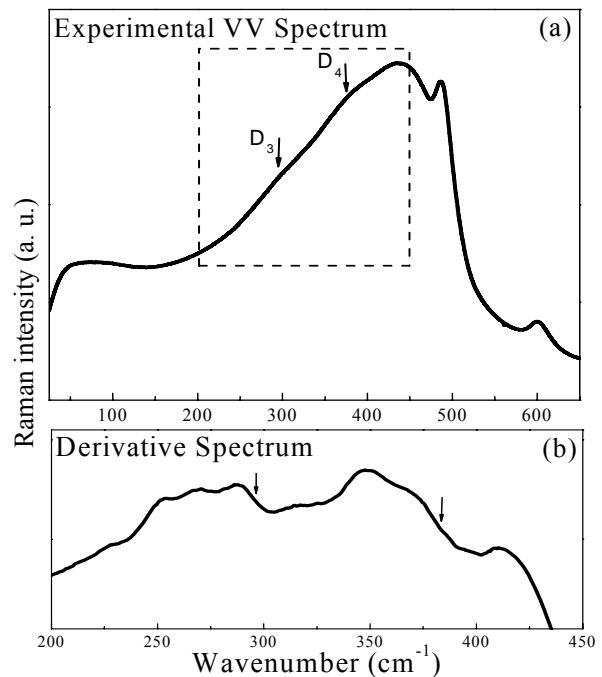


FIG.1. (a) Raman spectrum of silica (VV polarization configuration, 514.5 laser line, 90° configuration) with 17h of accumulation time. Arrows denote the position of the bumps visible on the rising edge of R-band. Dashed frame is the spectrum region derived in (b). (b) Derivative of the dash-enclosed part of the Raman spectrum of SiO_2 , allowing accurate determination of the position of the bumps (indicated by arrows).

Figure 1 (a) displays the $25\text{-}650\text{ cm}^{-1}$ frequency range of the VV polarized Raman spectrum of SiO_2 , obtained on the Jobin-Yvon spectrometer, with the Ar^+ 514.5 nm laser line, in macro- right angle configuration. This spectrum was acquired with a very long acquisition time (17h) in order to improve the signal-to-noise ratio. One can see, added to the well-known boson peak, R-band, D_1 and D_2 bands, two supplementary bumps, near 300 and 400 cm^{-1} . These bumps are rather broad and then they cannot give any detectable inflexion point on the rising edge of R-band if measurement is done with smaller acquisition times. As these bumps remain very small, possibility of any artifact in the experiment have been checked exhaustively: a first test to perform when recording such small and broad features is to check if there is no effect on non-uniform lightening on the CCD detector, by shifting the spectrograph of a small value: a non-uniform lightening stays at the same pixels whereas a real spectral feature shifts of pixels, to stay at the same wavenumbers. It was checked here that the two bumps are constant in wavenumbers. Other checks were done, to unambiguously establish that these bumps are intrinsic to the Raman response of silica. (i) Measurements were also done on the Renishaw Invia spectrometer (backscattering geometry and micro-Raman configuration) (ii) two other laser excitation lines were tried, i.e., 457 nm and 633 nm . (iv) Measurements with the Leica microscope

(Invia spectrometer) were done with two objectives (x20 and x50) in order to check the effect of numerical aperture and the possible subsequent changes in light polarization (v) changes of size of sample (from thickness of 1cm to 1mm), to check any interference or reflection effect between opposite faces. All these check measurements (all done with very long acquisition times) have confirmed the spectrum of figure 1(a) with its bumps. To determine more precisely the bump positions, it is useful to see the derivative of the spectrum (Figure 1(b)), much more sensitive to small features. The derivation was performed by the algorithm comprised in Microcal OriginPro8.1 software, with a Savitzky-Golay smoothing. The maximum of a peak in the original curve corresponds in the derivative curve to a zero value, or crossing through the baseline in the case of a peak superimposed to a broader and more intense feature. The bumps positions can then be determined rather precisely from figure 1(b): ≈ 295 and ≈ 380 cm^{-1} , the uncertainty being about 5 cm^{-1} . Hereafter they will be called respectively D_3 and D_4 bands by analogy with the D_1 and D_2 bands.

Now that the presence of both $D_3 \approx 295$ and $D_4 \approx 380$ cm^{-1} bands are established and even if to our knowledge, they were never reported explicitly before, one can remark that in some papers, the reported spectra have presumably exhibited them (¹³⁻¹⁴ for instance, among the most recent ones). Nevertheless, we underline that these features are very smooth compared to the underlying band and it was absolutely necessary to take specific acquisition times and to check for any possible artifact due to the experimental setup, as done in the present study. Above we have introduced that existence of numerous contributions to the Raman activity are expected in the R-band frequency region. Consequently, the possibility to fix the frequency of two of them has got considerable interest in the discussion of silicates structure.

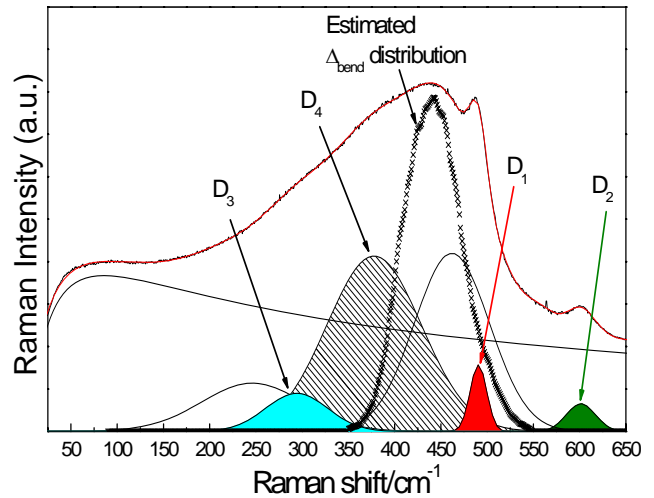


FIG.2. Deconvolution of the Raman spectrum of Silica (more details are given in the text).

In Figure 2, we present a new classic deconvolution of the spectrum. Generally, deconvolution results are dependent of the chosen band shapes and we have performed several tries: Figure 2 pictures one of these tries, where we have used a log normal shape for the boson peak, Lorentzian shapes for the D_1 and D_2 bands and Gaussian shapes for others. As one can see, additionally of the $D_2 \approx 605$ cm^{-1} , $D_1 \approx 495$ cm^{-1} , the ≈ 465 cm^{-1} band (maximum of the R-band), the $D_4 \approx 380$ cm^{-1} new feature, the $D_3 \approx 295$ cm^{-1} new feature and the boson peak, a band closed to 245 cm^{-1} is necessary in order to fit the full Raman activity in this wavenumbers region. In fact, this latter additional contribution is a common result of all the deconvolutions that we have performed (not shown here).

First, we note that these frequencies do not coincide with those of any of the natural SiO_2 crystalline polytypes (quartz, cristobalite, tridymite, stishovite, coesite)¹⁵. Second, frequency of the δ_{bend} (SiOSi) bending dynamic was successfully connected to the value of (SiOSi) angle (θ) through simple effective force constant models^{10, 11}. Therefore, consideration of the D_1 and D_2 bands through these models assign them as δ_{bend} dynamic of (SiOSi) bridges with different θ . In fact, in the specific case of 3-MR and 4-MR, the (SiOSi) bridges forming the rings are vibrating in phase leading to a “breathing” dynamic of the rings poorly coupled with their environment. The 3- and 4-MR rings appear then obviously in the Raman spectrum despite their very small amount obtained from different calculations^{7, 16}: around one ring of each specie for more than 500 SiO_4 tetrahedra according to Umari *et al*⁷. Then, if we consider, in one hand the (SiOSi) bridges in larger ($n \geq 5$) SiO_4 membered rings (hereafter denoted 5+MR) and, in other hand the widely observed and calculated θ distribution¹⁷⁻¹⁸, one can assign part of the R-band to δ_{bend}

dynamic of (SiOSi) bridges in 5+MR. Thus, the spectral signatures of larger rings are expected to be certainly broader than D_1 and D_2 , and lying at lower wavenumbers than these lines. In fact, in many of the amorphous SiO_2 calculated densities of states available in the literature (see for instance^{16, 19, 7}), one can see peaks or clear shoulders lying in the wavenumbers range of those evidenced in the present paper. Obviously, calculated features of large structures such as 5+MR will exhibit lower linewidths than experimental ones, at least as the limited number of atoms in numerical approaches hardens a good description of coupling between different oscillators. Besides, we assume that the rest of the Raman activity comes from the scissoring modes introduced in ref 12. In order to illustrate the spectral consequence of the θ distribution, in the following, we consider the (SiOSi) angle distribution calculated by Yuan et al.¹⁷. This calculation is consistent with NMR characterization of silica¹⁸ and gives (SiOSi) angle distribution centered to 147° with a full width at half maximum 23-30°. From the θ distribution, the induced frequency distribution in the Raman signature of (SiOSi) δ_{bend} can be estimated by used of the Effective Force Constant model of Lucovsky¹⁰, with the frequency of the highest VV Raman doublet as frequency of the (SiOSi) asymmetric stretching that is also active in IR¹². The distribution in frequency obtained is pictured by black crosses in Figure 2. In this calculation, the (SiOSi) δ_{bend} frequency for $\theta = 147^\circ$ is assumed to be at the 435 cm^{-1} maximum. These assumption give an angle of $\approx 128^\circ$ at the 3-MR frequency, consistent with others recent demonstrations²⁰. One can see that above estimated δ_{bend} frequency distribution merges on both $D_4 \approx 380$ and $\approx 465 \text{ cm}^{-1}$ bands. Then, one of the most plausible structural elements that can be connected with them are effectively the 5+MR. In fact, one knows from molecular dynamics that the ring statistics in silica is dominated by such rings (between 5 and 10), whereas 3-MR and 4-MR, marginal in the statistics, appear obviously in the Raman spectrum due to their strong decoupling from the bulk of the density of states. One SiO_2 crystalline structure is known to exhibit a large palette of different rings, that is silicalite -1-F¹⁴ (a SiO_2 -based zeolite, with 4-, 5-, 6- and 10-MRs). The Raman spectrum of silicalite is dominated by a sharp and intense line located at 380 cm^{-1} and a second one just below 300 cm^{-1} . These values coincide with those of D_3 and D_4 evidenced in the present results. Moreover, the remaining line at 445 cm^{-1} is presumably also visible in the silicalite 1F spectrum. Therefore, one can think to assign the full-set of lines used here to describe the silica Raman response (from 200 to 450 cm^{-1}) to vibration of different MR rings (presumably by decreasing order of frequencies, 5-, 6-, 7, and more -MR). In an other hand, the “breathing” nature of the small rings dynamic at the origin of sharp well-defined D_1 and D_2 bands is difficult to be taken account in the case of larger rings that are undoubtedly more distorted and coupled with their environment. We postulate

that reality of the Raman signature of δ_{bend} dynamic of (SiOSi) bridges should be between these two extreme cases: broad R-band due to the distribution in θ , and discrimination of the $D_4 \approx 380 \text{ cm}^{-1}$ and $\approx 465 \text{ cm}^{-1}$ wavenumbers bands due to the presence of rings patterns. Therefore, this view allows an assignment of the two $D_4 \approx 380 \text{ cm}^{-1}$ and $\approx 465 \text{ cm}^{-1}$ bands to (SiOSi) δ_{bend} in 5+MR. Besides, the lowest wavenumbers bands ($\approx 245 \text{ cm}^{-1}$ and $D_3 \approx 295 \text{ cm}^{-1}$) can thus be assigned to δ_{scis} and Δ_{scis} .

Above we have discussed a “classical deconvolution”. A rigorous discussion of the bands assignment containing band-shapes consideration needs to take also account of the Raman coupling parameter²¹ that was assumed to be mode and frequency dependent²². Such fine and complex discussion will be published elsewhere, being beyond the scope of this short paper where we essentially want to highlight the presence beyond doubt of two distinguishable new Raman spectral features in the R-band of silica: $D_3 \approx 295 \text{ cm}^{-1}$ and $D_4 \approx 380 \text{ cm}^{-1}$.

1. F. L. Galeener and G. Lucovsky, Physical Review Letters **37** (22), 1474-1478 (1976).
2. G. Lucovsky and F. L. Galeener, Journal of Non-Crystalline Solids **35-6** (JAN-), 1209-1214 (1980).
3. A. Pasquarello and R. Car, Physical Review Letters **80** (23), 5145-5147 (1998).
4. J. Burgin, C. Guillon, P. Langot, F. Vallee, B. Hehlen and M. Foret, Physical Review B **78** (18), 9 (2008).
5. J. C. Phillips, Physical Review B **33** (6), 4443-4445 (1986).
6. Thi Thao To, D. Bougeard and K. S. Smirnov Journal of Raman Spectroscopy **39** (12), 1869-1877 (2008).
7. P. Umari, X. Gonze and A. Pasquarello, Physical Review Letters **90** (2) (2003).
8. J. P. Rino, I. Ebbsjo, R. K. Kalia, A. Nakano and P. Vashishta, Physical Review B **47** (6), 3053-3062 (1993).
9. K. Vollmayr, W. Kob and K. Binder, Physical Review B **54** (22), 15808-15827 (1996).
10. G. Lucovsky, Philosophical Magazine B-Physics of Condensed Matter Statistical Mechanics Electronic Optical and Magnetic Properties **39** (6), 513-530 (1979).
11. F. L. Galeener, Physical Review B **19** (8), 4292-4297 (1979).
12. G. Guimbretiere, A. Bouchet, V. Rodriguez, M. Couzi, D. Talaga, T. Buffeteau and L. Canioni, Journal of Physical Chemistry C **112** (46), 17906-17915 (2008).

13. D. D. Goller, R. T. Phillips and I. G. Sayce, *Journal of Non-Crystalline Solids* **355** (34-36), 1747-1754 (2009).
14. J. Haines, C. Levelut, A. Isambert, P. Hébert, S. Kohara, D. A. Keen, T. Hammouda and D. Andraut, *J. Am. Chem. Soc.* **131** (34), 12333-12338 (2009).
15. .
16. A. Rahmani, M. Benoit and C. Benoit, *Physical Review B* **68** (18) (2003).
17. X. Yuan and A. N. Cormack, *Journal of Non-Crystalline Solids* **319** (1-2), 31-43 (2003).
18. T. M. Clark, P. J. Grandinetti, P. Florian and J. F. Stebbins, *Physical Review B* **70** (6) (2004).
19. M. Grimsditch, A. Polian and R. Vogelgesang, *Journal of Physics-Condensed Matter* **15** (31), S2335-S2341 (2003).
20. B. Hehlen, *Journal of Physics-Condensed Matter* **22** (2) (2010).
21. R. Shuker and R. W. Gammon, *Physical Review Letters* **25** (4), 222-& (1970).
22. F. L. Galeener and P. N. Sen, *Physical Review B* **17** (4), 1928-1933 (1978).